Antenna Azimuth Bearing Model Experiment

H. McGinness
DSN Engineering Section

The concluding description of the test is presented and reasons given for expecting a long service life from a large-scale prototype.

I. Introduction

In *DSN Progress Report 42-53* (Ref. 1), a partial report was given on the performance of a reduced-scale model of an antenna azimuth bearing. This bearing is of the wheel and track type and employs a novel suspension of the wheel. The following article completes the description of the model tests and discusses various aspects of the design. It is necessary that the reader refer to the partial report (Ref. 1) in order to understand this concluding part.

II. Model Running Tests

For the first two series of tests the model turntable was supported by three pairs of wheels as shown in Figs. 1 and 2 of Ref. 1. The load per wheel was 5560 N and produced a nominal hertz stress of 86,184 (10^4) N/m^2, based upon the net width of the contact area, which is the wheel width minus twice the corner radius.

The first series of tests was run for 40.60 hours, half of which was in the clockwise direction. No lubricant was added to the track, but a reddish brown color developed on top of the wear strips over the portion contacted by the wheels. The same color developed on the wheel rolling surfaces. It was decided to regrind the wear strip upper surfaces and the wheel rolling surfaces before starting the second series of tests. Upon removal of the wear strips it was seen that there was fretting corrosion at the interface of the wear strips and their support ring. It was then obvious that fretting products had migrated through the wear strip mitered joints and accounted for the discoloration of the wheels and top surfaces of the wear strips. A photograph of a typical corroded wear strip and support ring section is shown in Fig. 1.

There was no evidence of spalling or other fatigue failure on either the wheels or wear strips; however, there were minute pits probably caused by small broken particles from the edges of the mitered joints. (Later it will be shown that this will not occur on the prototype.) Figures 2 and 3 are, respectively, photographs of a wheel surface and wear strip after 40.6 hours of running.

Before regrinding the wheels, their diameters were measured and it was estimated that their diameter reductions through wear did not exceed 0.008 mm. Approximately 0.050 mm of material was removed from the top surfaces of the wear strips and from the rolling surfaces of the wheels by regrinding. Before reinstalling the wear strips, various lubricants were put between them and the support ring. These are shown in Fig. 4.

The second series of tests was run for a total of 81.54 hours, approximately half of which was in the clockwise

direction. The total running time for the first two series of tests was 122.14 hours or 45869 revolutions of the turntable. There was no evidence of fatigue failure of the wheels or wear strips. During the second series some of the lubricants placed on the bottom surfaces of the wear strips were extruded through the wear strip mitered joints and smeared over the upper surfaces, thus producing an inadvertent lubrication of the wheel track surface. After 31.66 hours of the second series of tests, a track lubricator was installed on each end of each pair of wheels. The lubricator consisted of a cylindrical rod of oil-impregnated plastic (SKF POLYOIL) approximately 11 mm in diameter, one end of which was lightly spring-loaded against the wear strip. It is claimed that the very thin film of oil deposited soon hardens to a waxlike substance which serves as a wheel-track lubricator yet does not collect foreign objects as would a conventional oil. Such a device serves also to brush large foreign objects away from the wheel path.

After 49.13 hours of running the second series of tests, 10 of the wear strips were removed and examined for fretting. Only two of the several lubricants had successfully prevented fretting. The results are listed in Table 1. The fretted wear strips were cleaned, coated with Silver Goop, replaced, and the second series of tests was resumed and run for 32.41 hours more. All wear strips were then removed and examined. Qualitative results are listed in Table 2.

For the third series of tests the wear strips were cleaned by regrinding slightly on both top and bottom surfaces. The bottom surfaces of some were plated as indicated in Fig. 5, whereas the remaining seven had the proprietary product CORTEC VCJ-309, a white powdered substance, put at the interface with the support ring.

Each wheel assembly was modified by replacing each used pair by an unused single wheel.[1] The three wheels were then adjusted so that their tangential misalignment to the track was not more than 30 arcseconds. The ballast weights were then adjusted so that the reaction on each of the two opposite wheels was 8749 N and the reaction on the third wheel was 8913 N. These values include the small effect of centrifugal force when rotating at the speed of 375.55 turns per hour. These loads are approximately 1.60 times the wheel loads used during the first two series of tests. The value of 1.6 is obtained from Eq. (6) of Ref. 1 by setting the scale factor λ at 0.042. Thus when loaded to this value the model is of scale 0.042 from a wheel-track fatigue life standpoint.

The third test series was begun and run intermittently over five days for a total of 38.24 hours. Approximately half was in the clockwise direction. The wheels and wear strips were visually inspected and appeared to be free from pits and spalling. There were some abrasion marks near the edge of each wheel but these were caused by the wheels hitting one of the wear strip holddown screw heads.

Five of the wear strips were removed and examined. Numbers 5, 16 and 18, which were plated respectively with copper, nickel, and tin, had lost most of the plating and fretting corrosion occurred. The chromium plating on number 2 was intact and clean. All the others, which had CORTEC at the interface, looked very good with only small traces of fretting.

For the fourth series of tests each wheel loading was reduced to 5674 N and each wheel was deliberately misaligned by 40 arcminutes with respect to a track tangent line. The turntable was run for a total of 19.28 hours, 11.16 hours of which was in the clockwise direction. An examination of the wheels and wear strips revealed a small amount of spalling at four places on wear strip number 15. This was the first and only evidence of fatigue failure. The wear strips had undergone a total of 179.66 hours. The test conditions are summarized in Table 3.

III. Drag Resistance Tests

In addition to the drag resistance tests reported in Ref. 1, the following were made. All the track lubricators were removed and the drive chain disconnected. The turntable was pushed with a force gage located at a radius of 1.84 m. When the turntable was pushed at a comfortable walking speed the gage read between 57 and 45 N. Then the wheel alignment was restored to the original good alignment of within 30 arcseconds of perfection, and push tests made. The force gage read between 40 and 31 N. The measured rolling resistance coefficient f_m is defined as:

$$f_m = \frac{T}{WR} \tag{1}$$

where

T is the measured torque

W is the total weight on all wheels

R is the mean radius of the track

Using 17000 N for W and 1.77 m for R, the following are calculated:

$$f_{m\ aligned} = \frac{(1.84) \times \begin{matrix} 40 \\ 31 \end{matrix}}{17000\ (1.77)} = \begin{matrix} 0.0024 \\ 0.0019 \end{matrix} \tag{2}$$

[1] The drawings which show the detailed construction of the model are JPL drawings 9472187 through 9472198.

$$f_{m \atop \text{misaligned by 40 arcmin}} = \frac{(1.84) \times \frac{57}{45}}{17000\,(1.77)} = \frac{0.0035}{0.0027} \qquad (3)$$

From Eq. (8) of Ref. 1, the following corresponding theoretical coefficient f_T may be obtained:

$$f_T = f_1 + f_2 \frac{d}{D} + \mu \sin \theta \qquad (4)$$

where

f_1 is the factor for roller thrust bearings

f_2 is the factor for radial ball bearings on the wheel axis

μ is the coefficient of sliding friction

d is the wheel bearing bore diameter

D is the wheel diameter

Using the following values: $f_1 = 0.0011, f_2 = 0.0015, d/D = 0.30, \mu = 0.20$, sin 40 arcmin. = 0.0116, Eq. (4) yields:

$$f_{T \atop \text{aligned}} = 0.0011 + 0.0015\,(0.30) + 0.20\,(0.00015) = 0.0016 \qquad (5)$$

$$f_{T \atop \text{misaligned by 40 arcmin}} = 0.0011 + 0.0015\,(0.30) + 0.20\,(0.0116) = 0.0039 \qquad (6)$$

The results of (5) and (6) are to be compared to the results of (2) and (3) respectively. The comparison suggests that Eq. (4) applies reasonably well to a large bearing of this type.

IV. Static Tests

In order to demonstrate that the wheel suspension system would safely support considerably more than its nominal load, it was overloaded under the following conditions. All of the ballast weights were stacked together at the position shown on the vertical centerline of Fig. 1 of Ref. 1. There were a total of three properly aligned wheels supporting the turntable. The total ballast weight was 27376 N and the reaction of the wheel nearest the ballast was 19547 N. The turntable was rotated back and forth approximately ±3°. Under this load the wheel support flexure struts (see Fig. 2 of Ref. 1) were slightly bowed as measured by a straight edge. Upon removal of the ballast weights, the bowing disappeared. It was observed that under a small load of about 100 N there was a slight asymmetry of the wheel support housing with respect to the flexure struts, which implied that the wheel had rotated a small amount in order to contact the track perfectly. This means that the strut was slightly bowed initially and that additional load increased the amount of bowing. The calculated axial load in each of the four flexure struts was 5642 N and the calculated critical load was 7592 N. Thus each strut was loaded to 5642/7592 = 74% of its critical buckling load without any visible damage. Notice that this load of 19547 N on the wheel was 19,547/5560 = 3.51 times the nominal load caused by antenna deadweight.

An examination of the wheel rolling surface and the wear strip disclosed no visible damage, nor was there any apparent damage to the portland cement grout beneath the track in the vicinity of the overloaded wheel.

V. Evaluation of the Fretting

There are many conflicting effects in the phenomenon of fretting corrosion; therefore it is not possible to know whether it would tend to be more or less severe on the prototype than on the model. The following conditions would be different:

(1) The time required to accumulate 67471 turns of the prototype antenna would be approximately 67 years, whereas this number of model turns was made in 180 hours.

(2) The amplitude of relative motion between the bottom surface of the wear strip and its support ring would be more on the prototype; namely, it would be $1/\lambda$ times the model amount.

(3) The model tests were conducted in a temperature- and humidity-controlled room, whereas the prototype would be exposed to the weather.

(4) The surface finishes of the prototype may be different from those of the model.

Since every lubricant used at the model wear strip interface was substantially effective in reducing the amount of fretting, and some virtually eliminated fretting, it is believed that some of these would be effective on the prototype. It is recommended that metallic platings not be used because their effectiveness is sacrificial in nature and would eventually disappear.

In order to retain lubricative substances at the interface, the edges of the wear strips, including the mitered ends, should be sealed to the support ring with a flexible material such as silicone rubber. Such a seal would also exclude foreign abrasives and moisture.

VI. Methods of Retaining the Support Ring

The method of retaining the model support ring, or track, is described in Ref. 1. Circumferential walking was prevented by four equally spaced tangential links. One end of a link was bolted to the outer edge of the support ring and the other end bolted to the concrete foundation. It was intended that the grout placed against each side of the support ring cross section (see Fig. 6) would resist side forces induced by slightly misaligned wheels. The fact is that a section of the outer grout shoulder, approximately 80° in angular span, was broken away and allowed the track to be displaced outward by as much as 1.4 mm. It is now believed that a portland cement shoulder is not suitable for retaining the support ring against these induced side forces nor against radial forces caused by a temperature difference between the support ring and concrete foundation. The latter force was not present on the model but would exist on the prototype.

It is believed that any of the three following methods would successfully retain the support ring of the prototype. The first method employs 16 equally spaced tangential links which connect the support ring to the concrete foundation. These links prevent circumferential walking, allow free radial expansion from temperature differences, and restrain the support ring against side forces induced by any combination of misaligned wheels. A structural analysis of this link arrangement has been made and will be reported separately. The results show that all stresses and displacements will be small. This method does permit small relative radial displacements between the support ring and the grout beneath it, which may be deemed unacceptable.

In order to eliminate the relative movement between the support ring and grout, the second method (see Fig. 7) has a thin sole plate between the support ring and the grout. The bottom surface of the sole plate must be keyed to the grout with both circumferential and radial keys. Sixteen tangential links would be used just as in the first method. Then the relative radial movement would be between the support ring and sole plate. The use of a sole plate requires that the bottom of the support ring be flat and that the sole plate be pressed against it firmly before the grout is packed into place. Another disadvantage of this method and of the first method is that the tangential links must be attached to steel plates embedded in the concrete foundation and not attached directly to the concrete because the bearing stresses would be too great. Also there is the possibility of fretting corrosion occurring between the sole plate and support ring.

The third method (see Fig. 8) would eliminate all the tangential links and employ circumferential and radial keys welded to the bottom of the support ring. The circumferential key would be at the bottom center of the support ring. It would serve to prevent radial movement between the support ring and grout whenever there is a temperature difference between the two. Sixteen equally spaced radial keys would prevent track walking. A stress analysis shows that the additional grout stresses caused by the key forces could be made sufficiently small with keys of moderate size.

VII. Wear Strip Mitered Joints

The top surface of the support ring was originally smooth and flat and the thicknesses of adjacent wear strips were the same to within 0.005 mm. When the model first rotated at the rate of 375.55 revolutions per hour, the noise it produced was very low and was described as a gentle hum. However, the noise level increased rapidly with the elapse of testing time. At the end of the tests the noise was described as a loud drumming sound. When the model was slowly pushed by hand it was observed that the noise level was fairly low except when a wheel was traversing a mitered joint, at which time a clanking sound was made and the wheel assembly could be seen to wobble.

Early examination of the mitered joints showed that a peening action was occurring. As the effects of the peening increased, the noise and wheel wobble increased. It is now believed that there is an effective step at the joint, even though the adjacent wear strips are of the same thickness, caused by elastic deformation. Whether peening occurs probably depends upon whether yield stresses are exceeded. It will be shown in the following discussion that the material stresses during the traversing of a joint are dependent upon the velocity and that the relatively high speed model intensified these stresses. It is expected that the amount of wear strip peening near the joints would be much less or nonexistent on the prototype.

In order to obtain the velocity scaling factor needed, a simpler joint is analyzed, namely, one which is perpendicular to the track. In Fig. 9 the wheel is shown at the beginning and end (solid and dashed lines respectively) of a joint traverse. Also indicated in Fig. 9 is the circular arc path of the wheel center and its rectangular coordinates s and y. For very small values of the ratio of step height h to wheel radius R, the wheel center path can be approximated closely by the sinusoid:

$$y = h \sin \frac{\pi}{2\sqrt{2Rh - h^2}} S \tag{7}$$

Let

$$S = VT \tag{8}$$

where V is the constant horizontal velocity of the wheel center and t is the time. The substitution of (8) into (7) gives the vertical position coordinate of the wheel y in terms of the time t, namely,

$$y = h \sin \frac{\pi V}{2\sqrt{2Rh - h^2}} t = h \sin \Omega t \tag{9}$$

Figure 10 shows the single-degree-of-freedom model to be analyzed. In this model the step is assumed to be perpendicular to the motion of the wheel, whereas on the physical model the step was formed by a 45° mitered joint. The main reason for analyzing the simpler condition is to obtain proper velocity scaling factors, which may be used to indicate that the prototype will have lower stresses during a joint traverse, even though the static stresses in the prototype and model are the same.

The equation of vertical motion of the dynamic model shown in Fig. 10 is

$$M\ddot{x} = -K(x - h \sin \Omega t) \tag{10}$$

where $\ddot{x}$ is the acceleration of mass M.

Defining the natural frequency ω as:

$$\omega^2 = \frac{K}{M}, \text{ Eq. (10) becomes} \tag{11}$$

$$\ddot{x} + \omega^2 x = \omega^2 h \sin \Omega t \tag{12}$$

When the initial conditions are zero, the solution of (12) is:

$$\ddot{x} = \frac{h\omega}{\omega^2 - \Omega^2} (-\Omega \sin \omega t + \omega \sin \Omega t) \tag{13}$$

The vertical velocity and accelerations of mass M are as follows:

$$\ddot{x} = \frac{h\omega^2\Omega}{\omega^2 - \Omega^2} (-\cos \omega t + \cos \Omega t) \tag{14}$$

$$\ddot{x} = \frac{h\omega^2\Omega}{\omega^2 - \Omega^2} (\omega \sin \omega t - \Omega \sin \Omega t) \tag{15}$$

The valid range of time t for Eqs. (13) (14) and (15) is

$$0 \leqslant t \leqslant \frac{\sqrt{2Rh - h^2}}{V} \tag{16}$$

For the application of concern, namely, azimuth bearing wheels for large antennas, the wheel mass is very small in comparison to the antenna mass associated with one wheel M, so that the assumption of a massless wheel is justified. The physical model which was tested had large ballast masses almost directly above a wheel. The flexure plates supporting the wheel (see Fig. 2 of Ref. 1) constitute most of the flexibility in the system; therefore this single-degree-of-freedom mathematical model is suitable for obtaining approximations for the real accelerations. The force between the wheel and track during a joint traverse may be obtained by multiplying $\ddot{x}$ by the mass M since the wheel is assumed to be massless.

The wheel velocity of the prototype V_p, which would produce the same stresses during a joint traverse as was produced in the physical model, is obtained in the following discussion which is based upon the assumptions that the model and prototype static stresses are identical and that the joints are geometrically similar. The first assumption requires that the prototype mass M_p be equal to the model mass M_m divided by λ^2, where λ is the ratio between corresponding model lengths and prototype lengths. The subscripts m and p refer to model and prototype respectively.

The foregoing assumptions are:

$$M_p = \frac{M_m}{\lambda^2} \tag{17}$$

$$h_p = \frac{h_m}{\lambda} \tag{18}$$

$$R_p = \frac{R_m}{\lambda} \tag{19}$$

As a test will show, the required prototype velocity is:

$$V_p = \frac{V_m}{\sqrt{\lambda}} \tag{20}$$

Equation (15) refers either to model or prototype. By writing $\ddot{x}_p$ in terms of model parameters, all scale factors will cancel if the prototype velocity, as given by Eq. (20), is correct.

The spring constant K was obtained by determining the deflection of the wheel support flexures as shown in Fig. 2 of Ref. 1. The result is:

$$K = \frac{3AE}{l} \tag{21}$$

where A is the cross sectional area of one flexure element, E is the elastic modulus, and l is the length of each flexure element.

Assuming that the E's are the same for model and prototype and that the two are geometrically similar, K_p may be expressed:

$$K_p = \frac{3\frac{A_m}{\lambda^2}E_m}{\frac{l_m}{\lambda}} = \frac{3A_m E_m}{l_m}\frac{1}{\lambda} = \frac{K_m}{\lambda} \qquad (22)$$

Substituting (22) and (17) into (11) there is obtained:

$$\omega_p^2 = \frac{K_p}{M_p} = \frac{K_m \lambda^2}{\lambda M_m} = \omega_m^2 \lambda \qquad (23)$$

From Eq. (9) the expression for Ω^2 is:

$$\Omega^2 = \frac{\pi^2 V^2}{4(2Rh - h^2)} \qquad (24)$$

Substitute (18) (19) and (20) into (24) and obtain:

$$\Omega^2 = \frac{\pi^2 V_m^2}{\lambda 4\left(\frac{2R_m h_m - h_m^2}{\lambda^2}\right)} = \Omega_m^2 \lambda \qquad (25)$$

Now substitute (18) and (23) into equation (15) and obtain

$$\ddot{x}_p = \frac{\frac{h_m}{\lambda}\omega_m^2 \lambda \Omega_m \sqrt{\lambda}}{\omega^2\lambda - \Omega_m^2\lambda}$$

$$[\omega_m\sqrt{\lambda}\sin\omega_m\sqrt{\lambda}\,t_p - \Omega_m\sqrt{\lambda}\sin\Omega_m\sqrt{\lambda}\,t_p] \qquad (26)$$

The substitution of (18) (19) and (20) into (16) yields:

$$t_p = \sqrt{\frac{2R_m h_m - h_m^2}{\lambda^2}}\frac{\sqrt{\lambda}}{V_m} = \frac{t_m}{\sqrt{\lambda}} \qquad (27)$$

The substitution of (27) into (26) yields:

$$\ddot{x}_p = \frac{h_m \omega_m^2 \Omega_m}{\omega_m^2 - \Omega_m^2}[\omega_m \sin\omega_m t_m - \Omega_m \sin\Omega_m t_m] \qquad (28)$$

Thus the $\ddot{x}_p$ value, or acceleration, of the prototype as given by (28) is identically equal to (15) with subscripts m. Since (15) applies either to model or prototype and since (28) is equal to (15), it is clear that when the prototype velocity is as given by Eq. (20), the prototype acceleration is equal to that of the model.

The acceleration as given by (15) will now be evaluated for the model test conditions. The following values of the parameters are:

h = 0.051 mm

R = 25 mm

V = 1.117 m/sec.

$$K = \frac{3AE}{l} = \frac{3(0.0000242)(20)10^{10}}{0.057}$$

$$= 254\,631\,579 \text{ N/m}$$

$$M = \frac{5560}{9.8} = 567 \text{ kilograms}$$

$$\omega^2 = \frac{K}{M} = 449085 \text{ rad/sec}^2$$

$$\omega = 670 \text{ rad/sec}$$

$$\Omega^2 = \frac{\pi^2 V^2}{4(2Rh - h^2)}$$

$$= \frac{\pi^2 (1.117)^2}{4\,[2(0.025)(0.000051) - (0.000051)^2]}$$

$$\Omega^2 = 1{,}208{,}506 \text{ rad/sec}^2$$

$$\Omega = 1099 \text{ rad/sec}$$

$$t_{max} = \frac{\sqrt{2Rh - h^2}}{V}$$

$$= \frac{\sqrt{2(0.025)(0.000051) - (0.000051)^2}}{1.117}$$

$$t_{max} = 0.00142 \text{ sec}$$

The substitution of the above parameters into Eq. (15) yields:

$$\ddot{x} = \frac{0.000051\ (449085)\ 1099}{449085 - 1208506}$$

$$[670 \sin 670\ t - 1099 \sin 1099\ t] \quad (29)$$

$$\ddot{x} = -0.033\ [670 \sin 670\ t - 1099 \sin 1099\ t] \quad (30)$$

The maximum absolute value of the bracket term of (30), within the time range zero to 0.00142 second, is approximately 581 rad/sec. Therefore the maximum value of $\ddot{x}$ is:

$$\ddot{x} = -0.033\ [-581] = 18.99\ \text{m/sec}^2 \quad (31)$$

The additional wheel to track force, F_D, caused by this acceleration is obtained by multiplying it by the mass M, obtaining:

$$F_D = M\ddot{x} = 567\ (18.99) = 10767\ \text{N} \quad (32)$$

The total wheel force is obtained by adding the static force F_s to the dynamic force F_D, obtaining:

$$F_{total} = F_s + F_D = 5560 + 10767 = 16327\ \text{N} \quad (33)$$

The ratio of F_{total} to F_s is:

$$\frac{F_{total}}{F_s} = \frac{16327}{5560} = 2.93 \quad (34)$$

The wheel velocity of a certain prototype antenna is 0.05 m/sec. If the model is considered to be a 1/12-scale model of this prototype, the model wheel velocity would be, from Eq. (20)

$$V_m = \sqrt{\lambda}\ V_p = \sqrt{\frac{1}{12}}\ 0.050 = 0.0144\ \text{m/sec} \quad (35)$$

The appropriate value of Ω^2, is, from Eq. (24),

$$\Omega_1^2 = 202 \quad (36)$$

$$\Omega_1 = 14.2 \quad (37)$$

The appropriate value of the time range is from Eq. (16)

$$t_{1_{max}} = 0.111\ \text{sec} \quad (38)$$

The value of the acceleration $\ddot{x}_1$, is obtained from (15)

$$\ddot{x}_1 = \frac{0.000051\ (449085)\ 14.2}{449085 - 202}$$

$$[670 \sin 670\ t - 14.2 \sin 14.2\ t] \quad (39)$$

$$\ddot{x}_{1_{max}} = 0.000724\ [665] = 0.482\ \text{m/sec}^2 \quad (40)$$

The additional wheel to track force, F_{D1}, caused by this acceleration is

$$F_{D1} = M\ddot{x} = 567\ (0.482) = 273\ \text{N} \quad (41)$$

The total wheel force is obtained by adding the static force F_s to the dynamic force, F_{D1}, obtaining:

$$F_{1_{total}} = F_s + F_{D1} = 5560 + 273 = 5833$$

The ratio of $F_{1_{total}}$ to F_s is:

$$\frac{F_{1_{total}}}{F_s} = \frac{5833}{5560} = 1.049 \quad (42)$$

This value, which pertains to a model run at the appropriate speed, is to be compared to the equation (34) value of 2.936, which pertains to the actual model running speed. At the appropriate speed the static loading is increased by 4.9%, whereas at the speed at which the model was run, the static loading was increased by 193%.

The foregoing ratios of total load to static load were derived for a zero gap step perpendicular to the track. It is reasonable to believe that the same force ratio would apply to the case of a step in a mitered joint, although the stresses of the mitered joint are probably quite different. This may be seen by referring to Fig. 11. In Fig. 11(a), which shows the perpendicular step, the entire length of the wheel contact area will hit the step at one instant and the impact forces will be uniformly distributed over the length. In Fig. 11(b) is shown the mitered step. Here, one end of the contact area will first strike the step so that the impact forces will be concentrated near the edge of the wear strip. Peened areas were formed where the figure indicates. Figure 12 is a photograph which shows the worst peened joint. Most probably the yield stresses were exceeded in these areas. Generally the peened areas existed in pairs, which implies that a portion of the step was formed by elastic deflection of the loaded side of the joint. The major portion of the step, however, probably came from different thicknesses of adjacent wear strips.

In practice it is necessary to employ mitered joints. If finite gap perpendicular joints were used, the stresses at the free edges would be excessive and cause rapid wear and roughness.

The model was run at high rotational speeds in order to obtain a large number of turns in a few weeks of testing time. All static stresses matched those of the prototype. The wheel loads induced by steps at the wear strip mitered joints were intensified by the high testing speed. It is important to realize that had the model been run at the appropriate scaled speed, as given by Eq. (20), the wheel loads at the joints would have been much less, and it is believed these loads would have been approximately 4.9% more than for the loads existing at the joints at zero speed. The stresses near the joint at zero speed condition are not known, but are sure to vary considerably with the step size. Therefore it is important to maintain as small a step condition as is practical.

For the case of a zero step, the maximum shear stress τ can be estimated from Eq. (1) of Ref. 1, namely,

$$\tau = 0.179\sqrt{\frac{F_s E}{DL}} \tag{43}$$

where D is the wheel diameter, L is its length, F_s is the static load from one wheel, and E is the common elastic modulus of the wheel and track.

For the case of low wheel velocities, where the effect of dynamic loading at a mitered joint is minor, it will be instructive to form the ratio of the calculated shear stress to the shear yield and then compare this ratio to corresponding ratios of known successful designs. The wear strip material of the model had a tensile yield stress of 105000 (10^4) N/m^2. The shear yield may be taken as a certain percentage of the tensile yield, say 50% of it, thus obtaining 52500 (10^4) N/m^2 as the shear yield of the material. Using this together with the calculated stress from Eq. (43), the following ratio is obtained, which is applicable for the model when running at the appropriate low speed:

$$\left[\frac{\tau}{\tau_{yield}}\right]_{model} = \frac{0.179}{52500\ 10^4}\sqrt{\frac{5560\,(20)\,10^{10}}{(0.050)\,(0.0105)}} = 0.496 \tag{44}$$

The successful design with which the model will be compared is the radial bearing of the 64-m-diameter antenna which has been in service at DSS 14 for 15 years. Its wear strips have a material tensile yield of 69000 (10^4) N/m^2, or a calculated shear yield of 34500 (10^4) N/m^2. The wheel diameter, effective wheel length, and wheel force of this design are respectively 0.914 m, 0.101 m and 445000 N. Using Eq. (43) the following ratio is obtained:

$$\left[\frac{\tau}{\tau_{yield}}\right]_{\substack{radial\\ bearing}} = \frac{0.179}{34500\,(10^4)}\sqrt{\frac{445000\,(20)\,10^{10}}{(0.914)\,(0.101)}} = 0.509 \tag{45}$$

Since there has been no damage to the edges of the wear strip mitered joints of the radial bearing assembly, and since its stress ratio as given by (45) is approximately the same as that of the model when the model runs at the appropriate low speed, it is concluded that had the model completed its large number of turns at low speed, there would not have been any peening at the ends of the wear strips. It should be emphasized that even after all the high speed turns the noisy model was operable in spite of the peening at the joint ends.

VIII. Conclusions

From the foregoing evaluation of the model tests the following conclusions are made:

(1) There is a tendency for a large-diameter circular track to move circumferentially and radially. If portland-cement-type grout is used for supporting the track, it is necessary to use auxiliary restraint devices to prevent the movement. It is believed that any of the three methods described would be satisfactory. Auxiliary restraint devices may not be required if another grout material, such as an epoxy-bonded grout, is used; but since this is not known, it is recommended that the auxiliary restraint devices be used with any grout material.

(2) The hardnesses of the wheels and wear strips apparently are sufficient to insure a long service life when used in conjunction with the wheel loading and wheel suspension system described. A detailed study of the test conditions summarized in Table 3 is necessary in order to make statistical predictions about the expected life of a prototype. The third series of tests, which was run at increased wheel loadings to compensate for scale effect, survived 14361 turns. It may be concluded that a three-wheel prototype would survive this number of turns.

(3) The wheel suspension survived an overload of 3.51 times its nominal load.

(4) The torque required to overcome the rolling resistance of the wheel can be estimated sufficiently well by using Eq. (8) of Reference 1.

(5) The traction capacity was found to be consistent with that from other sources.

(6) The infrequent transverse sliding of a nonrotating wheel across the track produces only negligible damage when the contact stresses and material properties are as herein stipulated.

(7) Fretting corrosion occurred on the model at the interface between the wear strips and the support ring. Two lubricants were found which almost eliminated fretting. Since it is probable that fretting would occur on a nonlubricated prototype, it is recommended that suitable lubricants be provided.

(8) The peening which occurred near the model wear strip ends is not expected to occur on the prototype because of velocity scale effect.

Reference

1. McGinness, H., "Antenna Azimuth Bearing Model Experiment," *The DSN Progress Report 42-53*, Jet Propulsion Laboratory, Pasadena, Calif., October 15, 1979.

Table 1. Qualitative comparison of lubricants used in controlling fretting corrosion at interface (the greatest amount of fretting from this group was small in comparison to the condition of no lubricant)

Wear strip number	Lubricant	Condition of interface after 49.13 hours of second series test,	Relative ranking class
2	Cortec	Very slight fretting, least amount	1
14	Silver Goop	Very slight fretting, least amount	1
10	Chassis grease	Small amount of fretting	3
3	Wheel brg. grease	Small amount of fretting	3
7	SAE 30 oil	Moderate amount of fretting	4
1	Darina No 2	Moderate amount of fretting	4
16	Mo S2	Considerable, but less than graphite	4
4	Graphite	Considerable fretting, greatest amount	5
5	Graphite	Considerable fretting	5
6	Graphite	Considerable fretting	5

Table 2. Qualitative comparisons of lubricants used in controlling fretting at interface

Wear strip number	Lubricant	Condition of interface after an additional 32.41 hours of second series test	Relative ranking class
2	Silver Goop[a]	Very slight amount of fretting, best class	1
14	Silver Goop	Very slight amount of fretting, best class	1
20	Silver Goop	Very slight amount of fretting, best class	1
10	Silver Goop[a]	Slight amount of fretting, next best class	2
17	Chassis grease	Considerable fretting, worst class	5
3	Silver Goop[a]	Small amount of fretting	3
13	Wheel brg. grease	Considerable fretting	5
7	Silver Goop[a]	Small amount of fretting	3
18	SAE 30 oil	Considerable fretting	5
11	SAE 30 oil	Considerable fretting	5
19	SAE 30 oil	Considerable fretting	5
7-2/3	SAE 30 oil	Considerable fretting	5
1	Silver Goop[a]	Moderate fretting	4
9	Darina no. 2	Considerable fretting	5
16	Silver Goop[a]	Moderate fretting	4
15	Dry MoS2	Considerable fretting	5
4	Silver Goop[a]	Small amount of fretting	3
5	Silver Goop[a]	Small amount of fretting	3
6	Silver Goop[a]	Small amount of fretting	3

[a]These employed a different lubricant during preceding 49.13 hours of testing, see table 1

Table 3. Summary of test conditions

	Load per wheel, N	No. of wheels	Lubrication between wheel and wear strip	Wheel misalignment, arcmin	Total running time, hr	Turns of antenna model
First series	5560	6	Products of fretting corrosion	Less than 0.50	40.60	15247
Second series	5560	6	Inadvertent lub. from substances beneath wear strip. Also polyoil	Less than 0.50	81.54	30622
Wheels replaced with new ones						
Third series	8913 8749	3	Polyoil plastic wiper	Less than 0.50	38.24	14361
Fourth series	5674	3	Polyoil plastic wiper	40	19.28	7241

Total turns of antenna model with first set of wheels was 45870. Each wheel of first set made 3256770 revolutions about wheel axis.

Total turns of antenna model with second set of wheels was 21602. Each wheel of second set made 1533742 revolutions about wheel axis.

Product of antenna model turns and number of wheels was 340026.

No evidence of fatigue damage to wheels.

Only wear strip No. 15 sustained spalling damage, and this occurred during fourth series of tests.

Fig. 1(a). Removed wear strip beside its support ring, showing fretting corrosion after 40.6 hours of running

Fig. 1(b). Enlarged view of portion of Fig. 1(a)

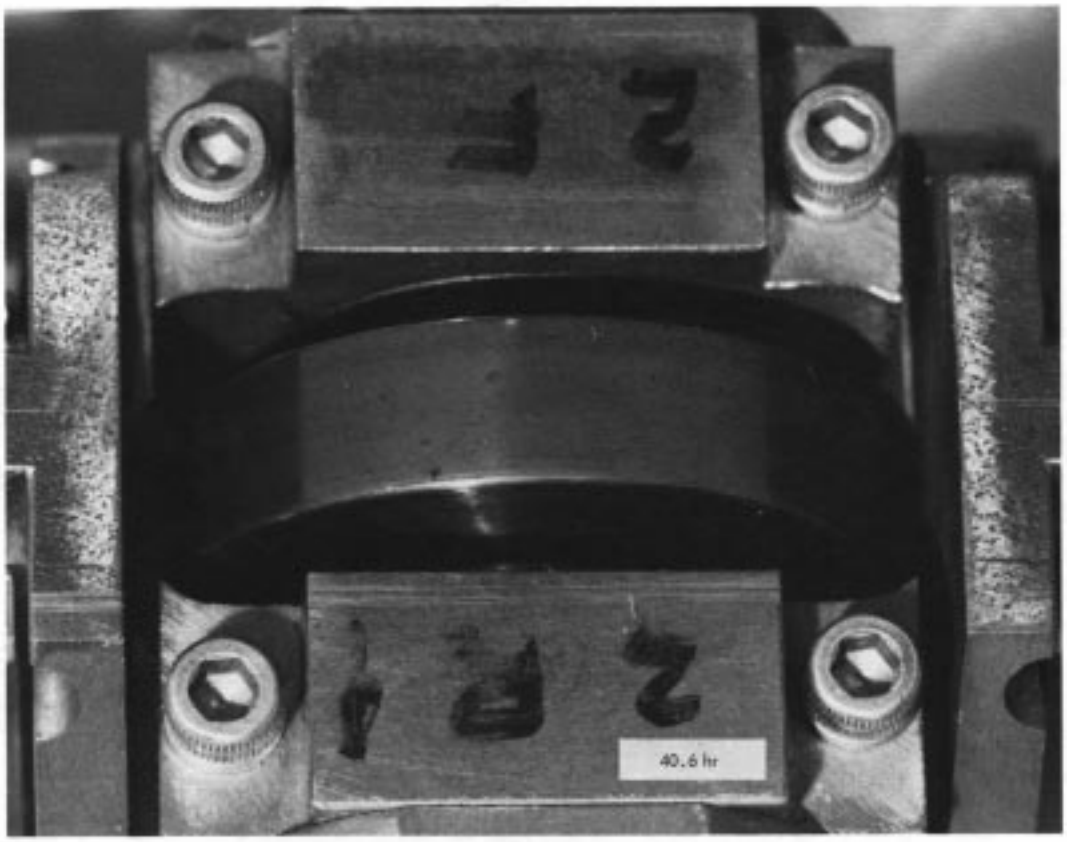

Fig. 2. Wheel surface after 40.6 hours of running

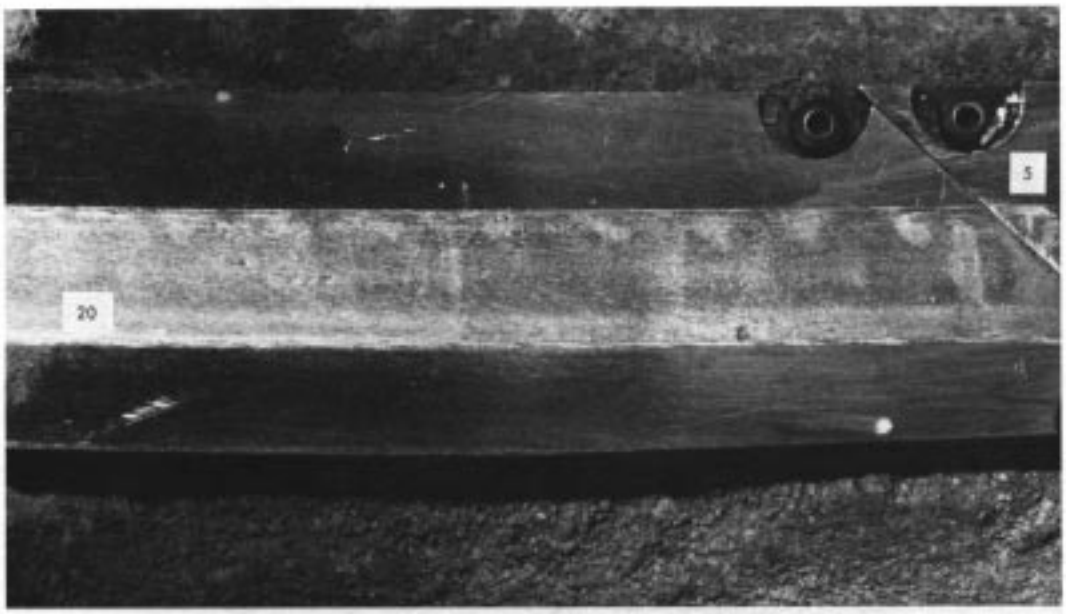

Fig. 3. Wear strip top surface after 40.6 hours of running

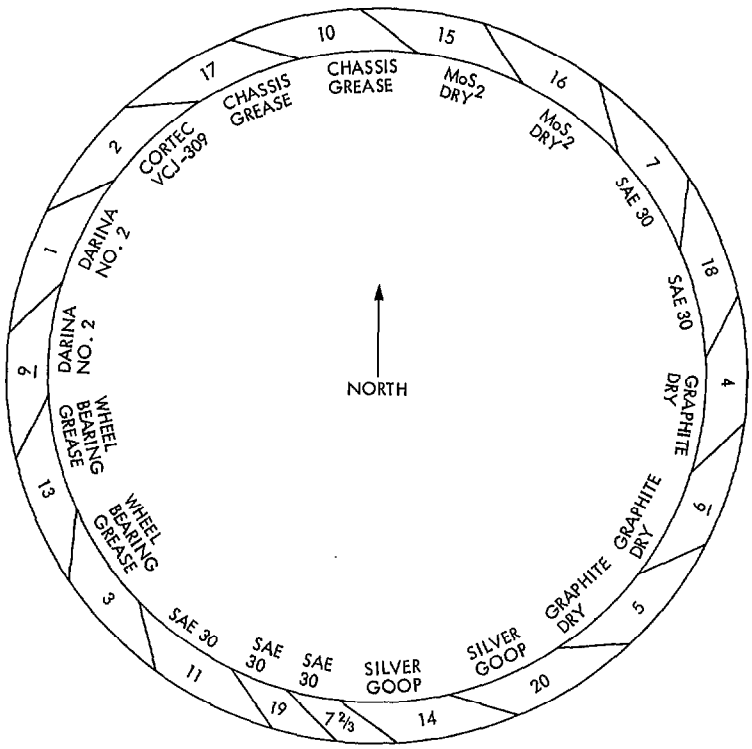

Fig. 4. Wear strip identification numbers and disposition of lubricants between wear strips and support ring

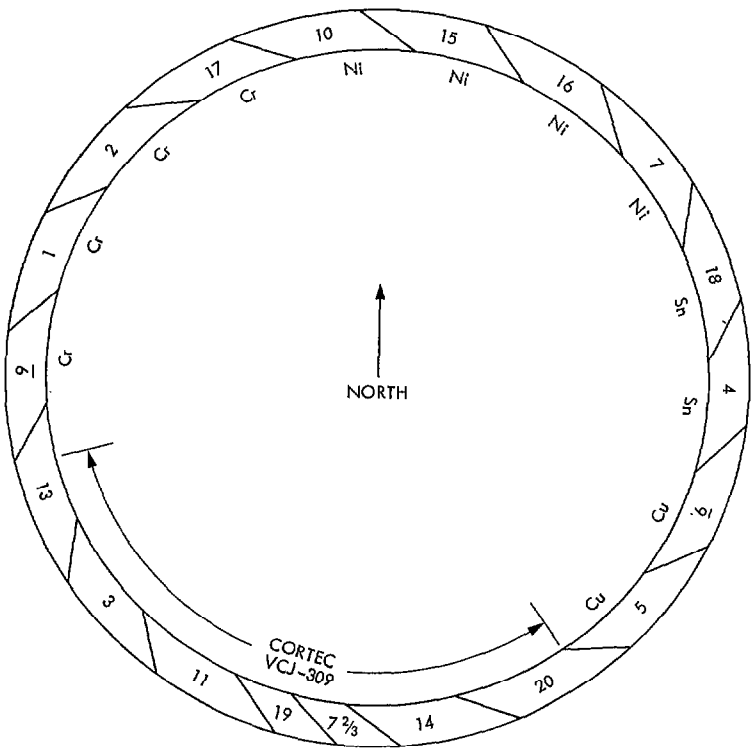

Fig. 5. Wear strip identification numbers and lubricant disposition for third series of tests

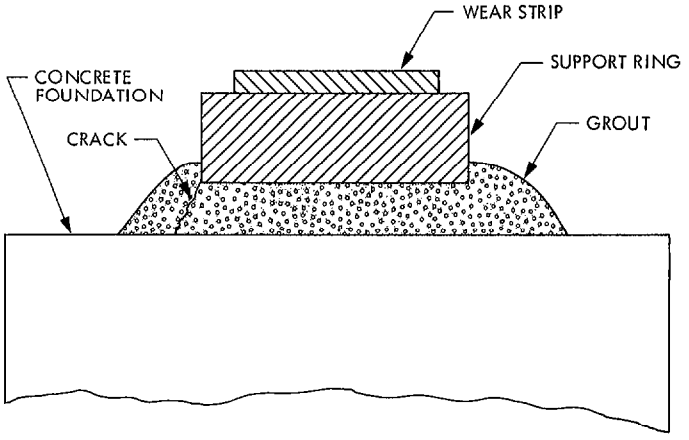

Fig. 6. Cross section of track showing cracked grout shoulder on outer side

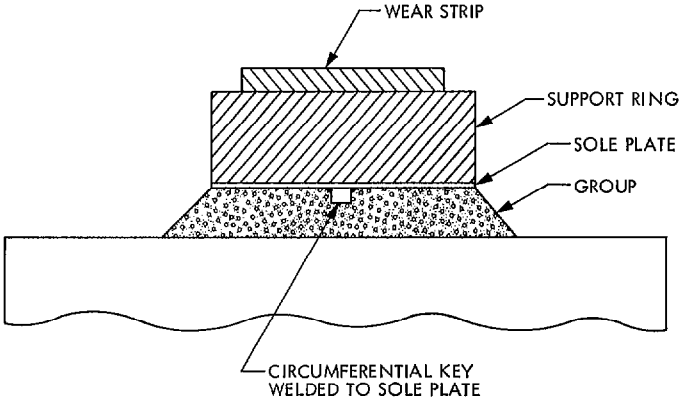

Fig. 7. Cross section of track showing addition of sole plate keyed to grout, method 2

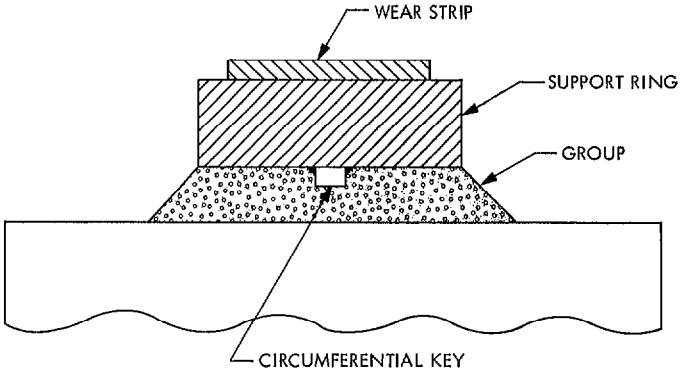

Fig. 8. Cross section of track showing circumferential key, method 3

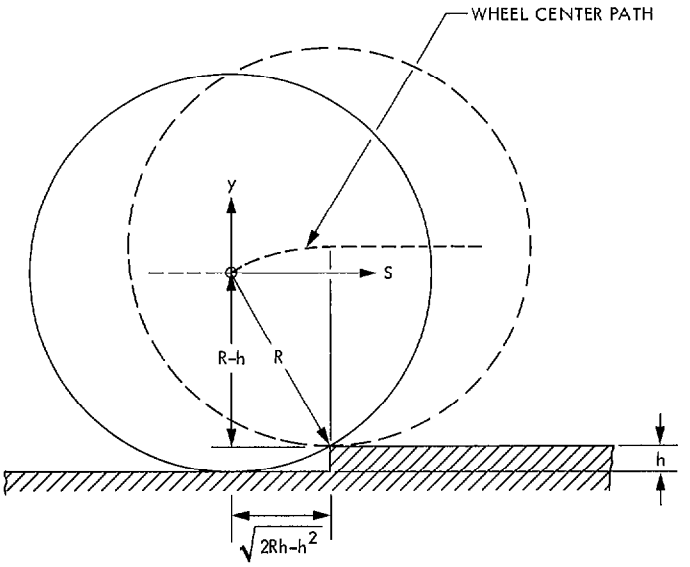

Fig. 9. Configuration of wheel against step at wear strip joint

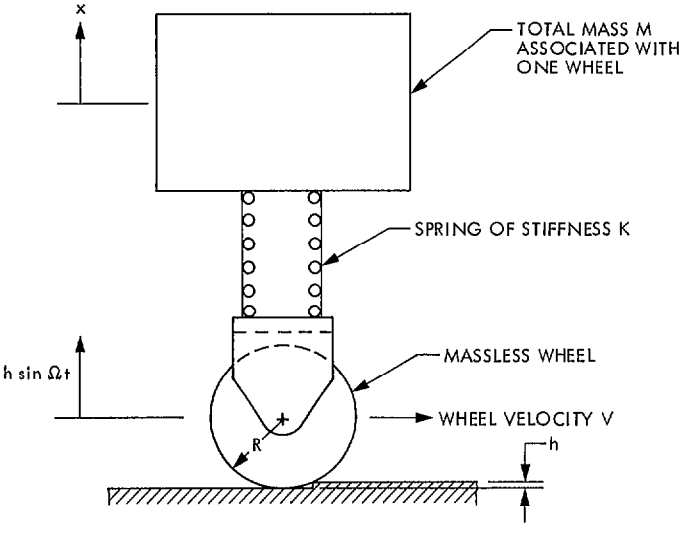

Fig. 10. The single-degree-of-freedom model analyzed

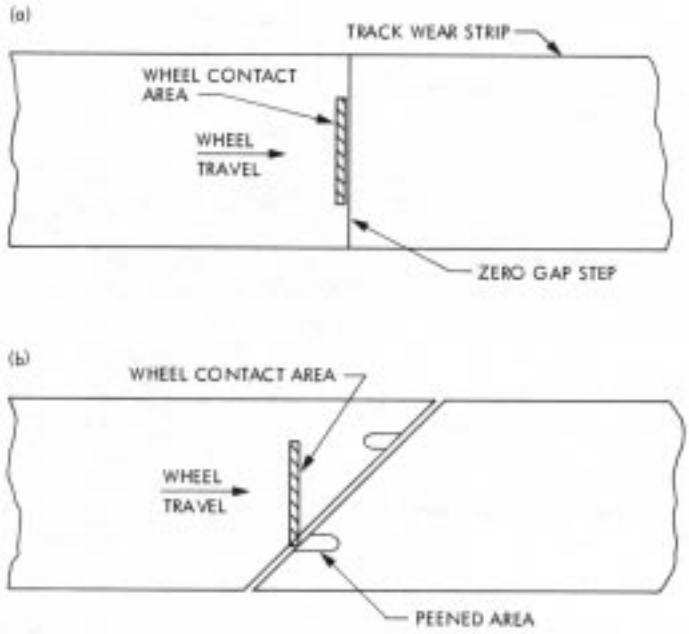

Fig. 11. Comparison of zero gap step perpendicular to track with a finite gap mitered step

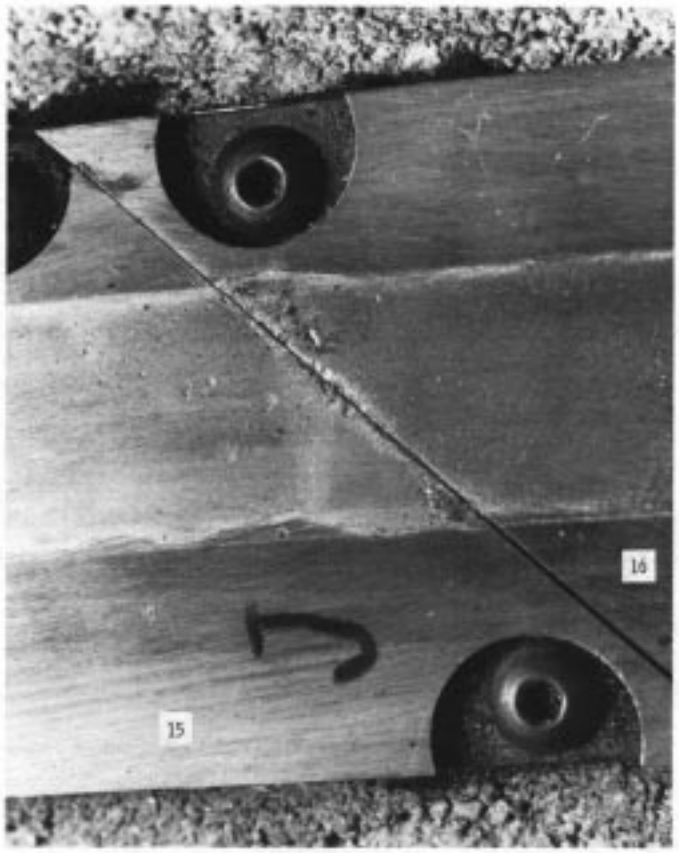

Fig. 12. Photograph showing peened areas at mitered point